



# Gold-enhanced Raman observation of chalcopyrite leaching

Gretel K. Parker\*, Gregory A. Hope, Ronald Woods

School of Biomolecular and Physical Science, Science, Environment, Engineering & Technology, Griffith University, 170 Kessels Road, Queensland 4111, Australia

## ARTICLE INFO

### Article history:

Received 6 August 2007

Received in revised form 29 April 2008

Accepted 29 April 2008

Available online 15 May 2008

### Keywords:

SERS

Chalcopyrite

Oxidation products

Sulfide ores

Leaching

## ABSTRACT

Gold decoration of chalcopyrite surfaces has been shown to stimulate surface enhancement of Raman scattering and this enables oxidation products, undetectable using normal Raman spectroscopy, to be investigated. Electroless deposition, sputtering and evaporative deposition facilitated SERS. *In situ* potentiodynamic investigations demonstrated similar oxidative product/s on the chalcopyrite surface in sulfate or chloride aqueous acid solutions. The product/s appeared to be amorphous and commenced S–S bonding in the transpassive potential region. The  $\nu_{SS}$  bands from the oxidized surface were broad and at a lower Raman shift than elemental sulfur, indicative of an aging metal-deficient remnant sulfide lattice. The oxidation product/s was not consistent with the formation of polysulfides or polythionates.

*Ex situ* investigations of oxidised chalcopyrite surfaces and model systems corroborated *in situ* data, in that the species detected were oxidation products of the chalcopyrite, rather than artifacts of sample preparation.

© 2008 Elsevier B.V. All rights reserved.

## 1. Introduction

Chalcopyrite [CuFeS<sub>2</sub>] is the most abundant copper-bearing mineral [1]. Hydrometallurgical processing offers the possibility of clean and contained mineral extraction, yielding both economic and environmental advantages. Sulfate-based leaching processes, particularly utilising ferric oxidants, are attractive because impurity management and control is well understood and copper winning from sulfate solutions is well established. However, ambient hydrometallurgical routes, particularly sulfate-leaching, are not well established for chalcopyritic ores due to hindered dissolution.

Under ambient acid leaching conditions, elemental sulfur and soluble iron and copper ions are the ultimate oxidation products. Elemental octasulfur is not generally considered to be responsible for passivation, although it may be responsible for hindered dissolution [2–5]. Proposed rate-inhibiting oxidation intermediates include covellite [6–9], metal-deficient polysulfides [3] (Cu<sub>1-x</sub>Fe<sub>1-y</sub>S<sub>2</sub>,  $x \ll y$ ,  $x+y \approx 1$  [10,11]; Cu<sub>0.8</sub>S<sub>2</sub> [6,12]) and ferric hydroxy sulfate by way of a disulfide phase [13–15]. The rate of leaching in chloride solutions at moderately elevated temperatures (80 °C) has been reported to follow parabolic kinetics, compared to parabolic kinetics in sulfate media; the anodic pre-wave responsible for product formation is observed in both systems [6,16–18]. The pre-wave product is likely responsible for the initial inhibition of chalcopyrite oxidation.

Normal Raman spectroscopy has been used in mineral oxidation investigations, and these studies have been reviewed by the authors in a companion paper [19]. Normal Raman spectroscopy is not sufficiently sensitive to detect thin product layers formed on corroding chalcopyrite, but has been used by the authors to establish bulk products in chalcopyrite oxidation, including a photosensitive Raman-inactive product phase which decomposed to polymeric sulfur under 442 nm irradiation, in addition to the expected cyclo-octasulfur. In order to establish the early oxidation products (i.e. the anodic pre-wave product) a more sensitive technique is required. To this end, we have employed surface-enhanced Raman scattering (SERS) via decoration with coinage metals, yielding detection limits to sub monolayer level, and including *in situ* studies of initial oxidative product formation. ‘Borrowing’ SERS is an established practice (e.g. see [20–22] and references therein) and has been used by the authors to investigate flotation collector–mineral interactions [23,24].

## 2. Experimental

Research-grade chalcopyrite specimens from Mt. Isa, Australia, Ward Scientific Establishment and Messina, Transvaal, South Africa, were used in this investigation.

Real-time electrochemical studies and SERS studies with gold were conducted on a Renishaw 100 system Raman spectrometer using 632.8 nm red excitation from a HeNe laser. The laser spot size was measured at ~50 μm with power at the sample measured at 6 mW (100% power). The scattered light was detected with a Peltier-cooled CCD detector with spectral resolution 2 cm<sup>-1</sup>.

\* Corresponding author. Tel.: +61 7 3735 3656; fax: +61 7 3735 7656.  
E-mail address: [g.parker@griffith.edu.au](mailto:g.parker@griffith.edu.au) (G.K. Parker).

The laser and scattered radiation were focused through an ultra-long working distance  $\times 20$  Olympus Plan FI lens ( $NA = 0.4$ ). Spectra were collected for 5–10 s during potentiodynamic scans, with a rest time of 1–2 s between scans. The grating was calibrated using the  $520\text{ cm}^{-1}$  silicon band. Spectral manipulations such as baseline adjustment, smoothing, fitting and normalisation were performed with GRAMS32 software (Galactic Industries, Salem, NH, USA). Band fitting was undertaken using mixed Gauss-Lorentz functions (ratio  $> 0.7$ ) with the minimum number of component bands required to achieve a  $R^2$  regression coefficient  $> 0.995$ .

Mineral electrodes for use with the Renishaw 100 electrochemical cell were prepared by attaching copper wire to chalcopyrite with silver-loaded epoxy, placing at the end of a glass tube for support, and, encasing the join with epoxy or polyester resin. The electrochemical cell had a conventional three-electrode configuration, consisting of a platinum counter electrode, a reference (Ag/AgCl/3.0 M KCl) electrode and a mineral working electrode. The electrolyte was purged in the cell by bubbling with high-purity nitrogen for at least 1 h prior to immersion of the mineral electrode. The cell was constructed from borosilicate glass and had an optically flat transparent window to facilitate collection of Raman scatter. Potential control was achieved using an ADInstruments potentiostat controlled by a MacLab/4e analog-digital converter interfaced with a PC running ADInstruments Echem software V1.5.2. The mineral surface was ground and rinsed with degassed doubly de-ionised (DDI) water under high-purity nitrogen immediately prior to submersing in the electrolyte. Electrolyte solutions were made using AR grade chemicals and DDI water ( $EC < 0.1\text{ }\mu\text{S cm}^{-1}$ ).

All potentials reported in this paper are against Ag/AgCl/3.0 M KCl reference.

For SERS studies of mineral surfaces during electrochemical investigations, surface enhancement was induced by deposition of gold films onto the mineral electrode surfaces. The efficacy of cementation, sputtering and evaporative deposition were compared. Solution deposition was accomplished by adding a small amount of 5 mM  $\text{AuCl}_4^-$  solution in 0.1 M KCl and 1 M HCl to the 0.1 M HCl electrolyte and maintaining the chalcopyrite electrode at its original open-circuit potential. Sputter coatings were formed utilising fine gold (99.9% Au) at sputter doses of  $25\text{ nm min}^{-1}$ . Evaporative deposition was achieved by thermally evaporating fine gold (99.9% Au) at 15 mA for 2–4 min, yielding discontinuous gold films. Coverage was in the range of nanometres ( $< 50\text{ nm}$ ), determined by simultaneously depositing onto glass slides and comparing with standards (based on weight of gold evaporated). Evaporative gold coating of samples was conducted under conditions of moderate to high vacuum ( $< 10^{-6}$  Torr).

Mineral samples for leaching and *ex situ* mapping were encased in clear polyester casting resin (1:100, v/v, FGI resin (Batch # BJ211037); methylethylketone peroxide hardener), cut with a diamond saw to produce an even surface for mapping and wet ground on P600, P800 and P1200 silicon carbide paper. Samples were not usually polished due to the possibility of thermal alteration of the sample surface, though when polishing was required a Struers polishing machine using 3 and  $1\text{ }\mu\text{m}$  diamond paste was utilised.

Raman spectral maps were collected on an InVia Raman spectrometer at Renishaw, UK. The excitation sources were 785 nm diode and 514.5 nm Ar ion lasers, operating at 1 mW and 2.5 mW, respectively, at the sample. Maps were collected in linefocus mode ( $\times 50$  Leica lens,  $NA = 0.75$ ) with 5 s accumulation at each point.

Scanning Electron Micrographs were collected using an FEI Quanta 200 instrument with a 10–12 mm working distance, a spot size of  $3\text{ }\mu\text{m}$  and beam energy of 15 kV and various detectors (Ever-

hart Thornley secondary electron detector, large field SE detector and SSD-BSE detector). Standardless EDX spectra were collected using a thin-window Si(Li) X-ray detector. Environmental SEM were collected using the Quanta 200 with a 10–12 mm working distance, spot size varying between 3 and  $5\text{ }\mu\text{m}$ , accelerating voltage varying between 7 and 20 kV and recorded using LFD and BSE detectors and pressure at 1 Torr of water vapour. Sputtering of samples was unnecessary for analysis under low-vacuum conditions.

X-ray photoelectron spectra were recorded on a Kratos Ultra Axis instrument with an Al  $K\alpha$  monochromated source,  $180^\circ$  hemispherical electron energy analyser of 165 mm mean radius and an 8-channeltron electron multiplier detector. Charge neutralisation was undertaken via the Kratos patented charge neutralisation system. Spectra were obtained at a source power of 150 W ( $15\text{ kV} \times 10\text{ mA}$ ) from a nominal incident spot of  $300\text{ }\mu\text{m} \times 700\text{ }\mu\text{m}$ . Survey scans were run at a constant analyser pass energy of 80 eV using 0.5 eV channel widths and a 100 ms dwell time per channel. High-resolution spectra were collected at a constant analyser pass energy of 20 eV, 0.1 eV channel widths and 200 ms dwell time. The spectrometer was calibrated using the C 1 s (285 eV) line, provided charging was negligible.

### 3. Results and discussion

#### 3.1. Sample characterisation and reference spectra

The chalcopyrite specimens used in this study contained primarily aluminosilicate impurities. The Mt. Isa material also contained detectable pyrite, chalcocite and cobaltite impurities ( $< 1\%$  total). The voltammetric behaviour of the specimens was examined and yielded similar results to those reported elsewhere [4,6,8], with an anodic pre-wave evident on the first sweep (max. current at  $\sim 0.6\text{ V}$ ) whose integrated charge was largely independent of sweep rate, sample origin, acid identity or acid concentration. The anodic pre-wave was virtually absent on subsequent sweeps provided the cathodic switching potential was not set too negative.

Fig. 1 displays the Raman spectrum of some reference compounds. The chalcopyrite Raman bands, due to lattice vibrations,

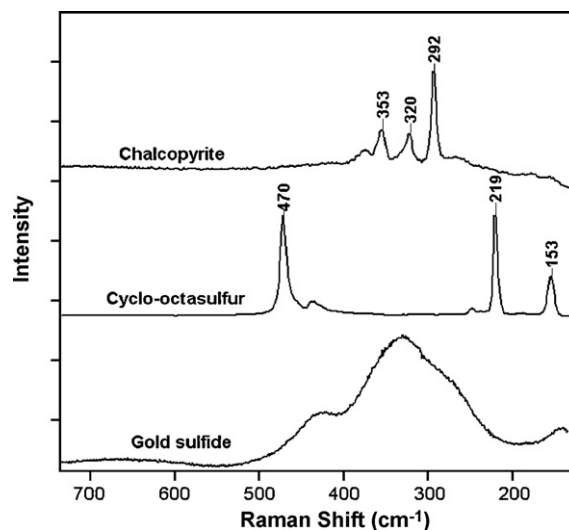


**Fig. 1.** Raman spectra of mineral and reference compounds: chalcopyrite (Excitation wavelength: 442 nm; irradiation density:  $0.102\text{ kW cm}^{-2}$ ;  $10\text{ s} \times 20$  accumulations), sulfur (Excitation wavelength: 442 nm; irradiation density:  $0.102\text{ kW cm}^{-2}$ ;  $10\text{ s} \times 1$  accumulations) and gold sulfide (Excitation wavelength: 632.8 nm; Irradiation density:  $0.0031\text{ kW cm}^{-2}$ ;  $10\text{ s} \times 100$  accumulations).

Download English Version:

<https://daneshyari.com/en/article/596471>

Download Persian Version:

<https://daneshyari.com/article/596471>

[Daneshyari.com](https://daneshyari.com)